

ORIGINAL ARTICLE

Neurofibromatosis-1 Heterozygosity Increases Microglia in a Spatially and Temporally Restricted Pattern Relevant to Mouse Optic Glioma Formation and Growth

Grant W. Simmons, PhD, Winnie W. Pong, PhD, Ryan J. Emnett, MS, Crystal R. White, MS,
Scott M. Gianino, MS, Fausto J. Rodriguez, MD, and David H. Gutmann, MD, PhD

Abstract

Whereas carcinogenesis requires the acquisition of driver mutations in progenitor cells, tumor growth and progression are heavily influenced by the local microenvironment. Previous studies from our laboratory have used Neurofibromatosis-1 (NF1) genetically engineered mice to characterize the role of stromal cells and signals to optic glioma formation and growth. Previously, we have shown that *Nf1*^{+/−} microglia in the tumor microenvironment are critical cellular determinants of optic glioma proliferation. To define the role of microglia in tumor formation and maintenance further, we used CD11b-TK mice, in which resident brain microglia (CD11b⁺, CD68⁺, Iba1⁺, CD45^{low} cells) can be ablated at specific times after ganciclovir administration. Ganciclovir-mediated microglia reduction reduced *Nf1* optic glioma proliferation during both tumor maintenance and tumor development. We identified the developmental window during which microglia are increased in the *Nf1*^{+/−} optic nerve and demonstrated that this accumulation reflected delayed microglia dispersion. The increase in microglia in the *Nf1*^{+/−} optic nerve was associated with reduced expression of the chemokine receptor, CX3CR1, such that reduced *Cx3cr1* expression in *Cx3cr1-GFP* heterozygous knockout mice led to a similar increase in optic nerve microglia. These results establish a critical role for microglia in the development and maintenance of *Nf1* optic glioma.

Key Words: Astrocytoma, Chemokine, Fractalkine receptor, Microenvironment, Optic glioma, Stroma.

From the Department of Neurology (GWS, WWP, RJE, CRW, SMG, DHG), Washington University School of Medicine, St Louis, Missouri; and Division of Neuropathology (FJR), Mayo Clinic Foundation, Rochester, Minnesota.

Send correspondence and reprint requests to: David H. Gutmann, MD, PhD, Department of Neurology, Washington University School of Medicine, Box 8111, 660 S Euclid Ave, St Louis, MO 63110; E-mail: gutmann@neuro.wustl.edu

This work was funded in part by a grant from the National Cancer Institute (U01-CA141549-01) to D.H.G. The Bakewell Neuroimaging Core is supported in part by the Bakewell Family Foundation and the National Institutes of Health Neuroscience Blueprint Interdisciplinary Center Core P30 Grant (NS057105 to Washington University). The High-Speed Cell Sorter Core is supported in part by a National Cancer Institute's Cancer Center Support Grant (P30 CA91842 to the Siteman Cancer Center).

Supplemental digital content is available for this article. Direct URL citations appear in the printed text and are provided in the HTML and PDF versions of this article on the journal's Web site (www.jneuropath.com).

INTRODUCTION

The concept that the tumor microenvironment plays instructive roles in oncogenesis and cancer growth has gained considerable traction during the past 10 years (1). In other cancers, stroma-tumor interactions involve immune system cells (leukocytes, mast cells, and macrophages) and fibroblasts, which secrete extracellular proteins, cytokines, and growth factors (2–5). Unlike other cancers, fibroblasts and mast cells are not relevant stromal cell types in brain tumors (gliomas), suggesting that other cell types may contribute to microenvironmental influences on central nervous system (CNS) tumorigenesis and growth. Moreover, the stromal signals that influence glioma formation and growth are likely distinct from those implicated in non-CNS cancers and may be regulated in spatial and temporal patterns during postnatal brain development.

Previous studies from our laboratory have used *Nf1* genetically engineered mouse (GEM) strains to define the role of the tumor microenvironment in glioma formation and growth. Neurofibromatosis-1 is a common tumor predisposition syndrome in which children are prone to the development of low-grade glial cell neoplasms (gliomas) along the optic pathway (optic pathway gliomas). These low-grade gliomas are classified as World Health Organization (WHO) grade 1 pilocytic astrocytomas and are typically found in the optic nerve and chiasm of children younger than 7 years (6). Children with NF1 are born with 1 nonfunctional copy of the *NF1* gene in all cells of their body (*NF1* heterozygosity; *Nf1*^{+/−}) but develop gliomas only upon loss of the one remaining functional allele in glial progenitor cells. To model this genetic condition in mice, we previously generated mice with *Nf1* inactivation in glial progenitors; however, none of these mice developed gliomas (7). In contrast, glioma formation was only observed in *Nf1*^{+/−} mice with glial cell *Nf1* inactivation, thus establishing an absolute requirement for *Nf1* heterozygosity in glioma formation (8). The observation that *Nf1* loss in glial progenitors is necessary, but not sufficient, for tumorigenesis supported the hypothesis that nonneoplastic *Nf1*^{+/−} cells provide a permissive environment required for glioma formation. By leveraging *Nf1* GEM strains with highly penetrant tumor phenotypes, we showed that microglia represented one of the critical cell types present in the tumor microenvironment of *Nf1* optic glioma mice (9).

Microglia have long been recognized as a major cellular constituent of the glioma microenvironment (10–13).

Rio-Hortega and Asua (14) first identified microglia in brain tumors in 1921; however, their role in glioma formation and continued growth (maintenance) remains unclear. In this regard, microglia may have antitumor activity (15, 16) or promote glioma growth by producing cytokines, such as interleukins 1 and 10, basic fibroblast growth factor, and transforming growth factor β (17–19). To define the role of microglia in glioma growth, we previously used 2 independent approaches to microglia inactivation in *Nf1* GEM optic gliomas. First, using minocycline to inactivate microglia in 10- to 12-week-old *Nf1* optic glioma mice, we found that reduced microglia activation, as assessed by morphological change, reduced tumor proliferation (20). Second, we identified that *Nf1*^{+/−} microglia, but not *Nf1*-deficient astroglial cells, exhibited hyperactivation of c-Jun-NH₂ kinase (JNK) such that treatment of *Nf1* optic glioma mice with a relatively nonselective pharmacologic JNK inhibitor attenuated tumor proliferation (21). These proof-of-principle experiments demonstrated that *Nf1*^{+/−} microglia inactivation decreased *Nf1* optic glioma proliferation in vivo, but the inhibitors used in these studies did not directly target microglia and may have had additional effects. Moreover, these studies did not address the importance of microglia during *Nf1* optic glioma development.

In the current study, we use a novel CD11b-TK transgenic mouse strain to ablate microglia genetically and demonstrate that microglia are important stromal cell types during gliomagenesis (tumor development) and for glioma maintenance. In addition, we define a spatially and temporally restricted window in which increased numbers of microglia are present in the *Nf1*^{+/−} optic nerve. We further demonstrate that this increase in microglia likely reflects impaired microglial dispersal during postnatal optic nerve development as a result of reduced CX3CR1 expression. Collectively, these findings establish a critical role for microglia in promoting tumor proliferation throughout gliomagenesis.

MATERIALS AND METHODS

Mouse and Human Specimens

Mice were used in accordance to established Animal Studies Protocols at the Washington University School of Medicine. *Nf1*^{flox/−}; *GFAP-Cre* (*Nf1*^{+/−}/*GFAP*CKO), *Nf1*^{flox/−}; *GFAP-Cre*; *CD11b-TK* (*Nf1*^{+/−}/*GFAP*CKO-TK), *CD11b-TK* (22), *Cx3cr1*^{+/−}/*GFP* (23), *Nf1*^{+/−}; *Cx3cr1*^{+/−}/*GFP*, wild-type (WT), and *Nf1*^{+/−} mice were all maintained on a C57BL/6 background. The *Nf1*^{+/−}/*GFAP*CKO optic gliomas lack the Rosenthal fibers and eosinophilic granular bodies that are characteristic of human pilocytic astrocytomas but otherwise closely resemble pediatric low-grade gliomas based on the presence of discrete optic nerve/chiasm masses composed of hyperproliferating astrocytes with large hyperchromatic nuclei, low proliferative indices, new blood vessel formation, microglia infiltration, Olig2-immunoreactive cells, and contrast enhancement on small-animal magnetic resonance imaging (8); there is no evidence of endothelial hyperplasia or necrosis.

Human tumor specimens were used in accordance with established guidelines under an active and approved human studies protocol. Human glioma specimens were studied

using 2 individual tissue microarrays developed at the Mayo Clinic Foundation and Washington University School of Medicine, as previously reported (24, 25). Nonneoplastic human brain samples from the neocortex were obtained from autopsy materials acquired under an approved human studies protocol at the Washington University School of Medicine.

Immunohistochemistry

Mice were perfused transcardially with 4% paraformaldehyde in 0.1 mol/L sodium phosphate buffer (pH 7.4). Optic nerves and optic chiasms were dissected and postfixed in 4% paraformaldehyde overnight at 4°C. All specimens were then processed for paraffin embedding and sectioning at the Ophthalmology Histology Core or the Histology and Microscopy Core at Washington University School of Medicine. Slides were deparaffinized in xylene and subjected to antigen retrieval. After the washing and blocking steps, sections were incubated overnight with rabbit anti-Iba1 (1:3000; Wako, Richmond, VA), mouse anti-Ki67 (1:500; BD Biosciences, San Jose, CA), or rat anti-CD34 (1:50; BD Biosciences) followed by incubation with biotinylated secondary antibodies (1:200; Vector Laboratories, Burlingame, CA) at room temperature (RT) for 1 hour. Immunoreactivity was visualized with the Vectastain ABC system and 3,3'-diaminobenzidine, Vector NovaRED, or Vector SG (Vector Laboratories).

All sections were photographed using a digital camera attached to a Nikon Eclipse E600 microscope (Nikon Instruments Inc., Melville, NY). For each optic nerve counted, 3 photographs were taken at a magnification of 10× for at least 4 mice/group, including the optic chiasm and the right or left optic nerve just anterior to the chiasm (Figure, Supplemental Digital Content 1, part A, <http://links.lww.com/NEN/A199>). For brainstem and neocortex regions, 4 photographs were taken at a magnification of 10× for at least 4 mice/group (Figure, Supplemental Digital Content 1, parts B, C, <http://links.lww.com/NEN/A199>). The total number of Iba1⁺ cells was quantitated in the mouse prechiasmatic optic nerves, chiasm, brainstem, and neocortex, as previously described, with the investigator blinded to the genotype and treatment (26). All Iba1⁺ cells were counted regardless of morphology (amoeboid vs ramified). In the human tumors, the number of Iba1⁺ cells was calculated as a percentage of the total number of nucleated cells.

Immunofluorescence

After transcardial perfusion with Ringer's solution (147 mmol/L NaCl, 4 mmol/L KCl, 2.2 mmol/L CaCl₂·2H₂O, with 2.5 USP U/mL heparin sodium injection, 0.02 mg/mL lidocaine HCl), WT mouse optic nerves and chiasms were dissected and postfixed in 4% paraformaldehyde overnight at 4°C. Tissues were cryoprotected in 30% sucrose in 0.1 mol/L sodium phosphate buffer (pH 7.4), embedded in OCT medium (Tissue-Tek, Miles, Inc., Elkhart, IN), cut into 10-μm sections in a cryostat, collected on Superfrost Plus slides (Fisher Scientific, Waltham, MA), and stored at −20°C. Slides were washed; permeabilized in 0.2% Triton X-100 in phosphate buffer; blocked; incubated overnight at 4°C with rabbit anti-Iba1 (1:2000), rat anti-CD11b (M1/70, 1:10; BD Biosciences), or mouse anti-Ki67 (1:500; BD Biosciences);

and followed by incubation with fluorescent secondary antibodies (1:200 goat anti-rat A488, goat anti-rabbit A568, or goat antimouse A488; Invitrogen, Carlsbad, CA) for 1 hour at RT. In all cases, no specific immunostaining was observed in the negative control samples. Images were acquired using an Olympus multichannel confocal microscope (Olympus America Inc., Center Valley, PA) in the Washington University Bakewell Neuroimaging Core Facility, and Image J image analysis software (<http://rsbweb.nih.gov/ij/>; Wayne Rasband, National Institute of Mental Health, Bethesda, MD) was used to obtain a single collapsed image from an optical stack.

Ganciclovir Treatment

Ganciclovir (GCV; Sigma-Aldrich, St Louis, MO) was dissolved in phosphate-buffered saline (PBS) and administered at a dosage of 50 mg/kg. For the experiments focused on determining the acute effects of microglia ablation on optic glioma proliferation, *Nf1*^{+/−}-*GFAP*^{CKO-TK} mice were divided into 2 groups: one group received daily intraperitoneal GCV injections for 2 weeks starting at 3 weeks or 3 months, whereas the other group received daily intraperitoneal injections of vehicle (PBS) starting at 3 weeks or 3 months.

Flow Cytometry

Microglia from mice were collected using previously described procedures with minor modifications (27). Briefly, for each experiment, optic nerves and chiasms harvested from 7 to 10 mice, transcardially perfused with Ringer's solution, were homogenized through a 70-μm nylon filter (Fisher Scientific), enzymatically digested in Hanks' buffered salt solution without calcium and magnesium containing 0.05% collagenase I (Sigma-Aldrich), 0.1 μg/mL $\text{N}\alpha$ -tosyl-L-lysine chloromethyl ketone hydrochloride (TLCK; Sigma-Aldrich), 0.01 mg/mL bovine deoxyribonuclease I (DNase I; Sigma-Aldrich), 10 mmol/L HEPES buffer (pH 7.4) for 1 hour at RT, and filtered through a 40-μm nylon filter (Fisher Scientific). Brainstem specimens were similarly processed to obtain cells for flow cytometry controls. A discontinuous Percoll gradient (Amersham/GE Healthcare, Waukesha, WI) of 30%, 37%, and 70% allowed for collection of an enriched macrophage and microglia sample from the 37% to 70% interface. Alternately, magnetic cell sorting using CD11b microbeads after myelin removal (Miltenyi Biotec, Bergisch Gladbach, Germany) was used to extract the CD11b⁺ microglia population. After Fc blocking with a CD16/32 antibody (BD Biosciences), cell surface staining was performed with anti-CD45-APC (30-F11; BD Biosciences) and anti-CD11b-PerCP-Cy5.5 antibodies. In some experiments, cells were fixed and permeabilized with the BD Cytofix/Cytoperm Fixation/Permeabilization Kit (BD Biosciences) and then stained with CD68-R-PE (FA-11; AbD Serotec, Oxford, UK) or rabbit anti-Iba1 (Wako) conjugated to R-PE using the Zenon Rabbit IgG Labeling Kit (Molecular Probes, Invitrogen). Isotype and fluorescence minus one (FMO) controls were used to determine nonspecific staining. Flow cytometry data were collected on a BD FACScan flow cytometer retrofitted with a second laser (Cytek, Fremont, CA) using CellQuest (BD Biosciences) and Rainbow software (Cytek) in the High-Speed Cell Sorter Core Facility at the

Siteman Cancer Center, Washington University, and data were subsequently analyzed using FlowJo (Tree Star, Inc., Ashland, OR). Viable cells were gated by Forward Scatter (FSC) and Side Scatter (SSC) characteristics, and the appropriate controls were used for compensation and to determine negatively and positively stained populations, as previously described (28).

Quantitative Reverse Transcription–Polymerase Chain Reaction

Real-time polymerase chain reaction (quantitative PCR, qPCR) was performed using SYBR Green detection according to the manufacturer's instructions. Total RNA was extracted from *Nf1*^{+/−} and WT optic nerve using TRIzol. Complementary DNA was synthesized from total RNA samples using the Ominiscript kit (Qiagen, Alameda, CA). Amplification was performed in 96-well plates in a real-time sequence detection system instrument (CFX96 Real-Time System; Bio-Rad, Hercules, CA). Primer sequences for *Cx3cr1* were 5'-AGGCCTGT TATTGGCGACAT-3' (forward) and 5'-AGCGAGGACCA CCAACAGATT-3' (reverse). Primer sequences for *Cx3cl1* were 5'-AAATGGGTCCAAGACGCCATGA-3' (forward) and 5'-ACATTGTCCACCCGCTTCTCAA-3' (reverse). Bio-Rad CFX Manager software was used to convert the fluorescent data into cycle threshold (CT) measurements. The ΔΔCT method was used to calculate changes in fold expression relative to WT optic nerve using β-actin as an internal control.

Statistical Analyses

Student *t* tests, along with Grubbs test to determine outliers, were performed for all statistical analyses. Mean and SEM were used for all graphs. For all experiments involving cell quantitation, the investigators were blinded to mouse genotype and treatment.

RESULTS

Increased Microglia in NF1-Associated Pilocytic Astrocytomas

Several previous studies have reported increased numbers of microglia in human gliomas, constituting as many as a third of all cells in glioma biopsies (10–13). We also found a 2-fold increase in the percentage of Iba1-positive cells (microglia) in high-grade human astrocytomas (Figs. 1A, B). Previous studies have suggested that Iba1 is a more selective marker of brain microglia in both human (29) and rodent tissues (30). By contrast, anti-CD68 antibodies label resident brain microglia (CD68⁺, CD11b⁺, CD45^{low} cells), (31, 32), lymphocytes (CD68⁺, CD11b^{+/−}, CD45^{high}) (33, 34), neutrophils (CD68⁺, CD11b⁺, CD45^{high}) (35, 36), dendritic cells (CD68⁺, CD11b⁺, CD45^{high} cells) (37, 38), and bone marrow-derived monocytes (CD68⁺, CD11b⁺, CD45^{high} cells) (32, 39). Similar percentages of microglia were generally found in WHO grade 1 low-grade gliomas as in the high-grade tumors, but NF1-associated pilocytic astrocytomas (NF1-PA) had higher percentages of microglia than their sporadic counterparts (SP-PA) ($p = 0.0008$) (Figs. 1A, C).

Because previous reports used CD68 as a marker for microglia in brain tumors (40, 41), we analyzed numbers of CD68⁺ cells in the PA tumors. There was a trend toward

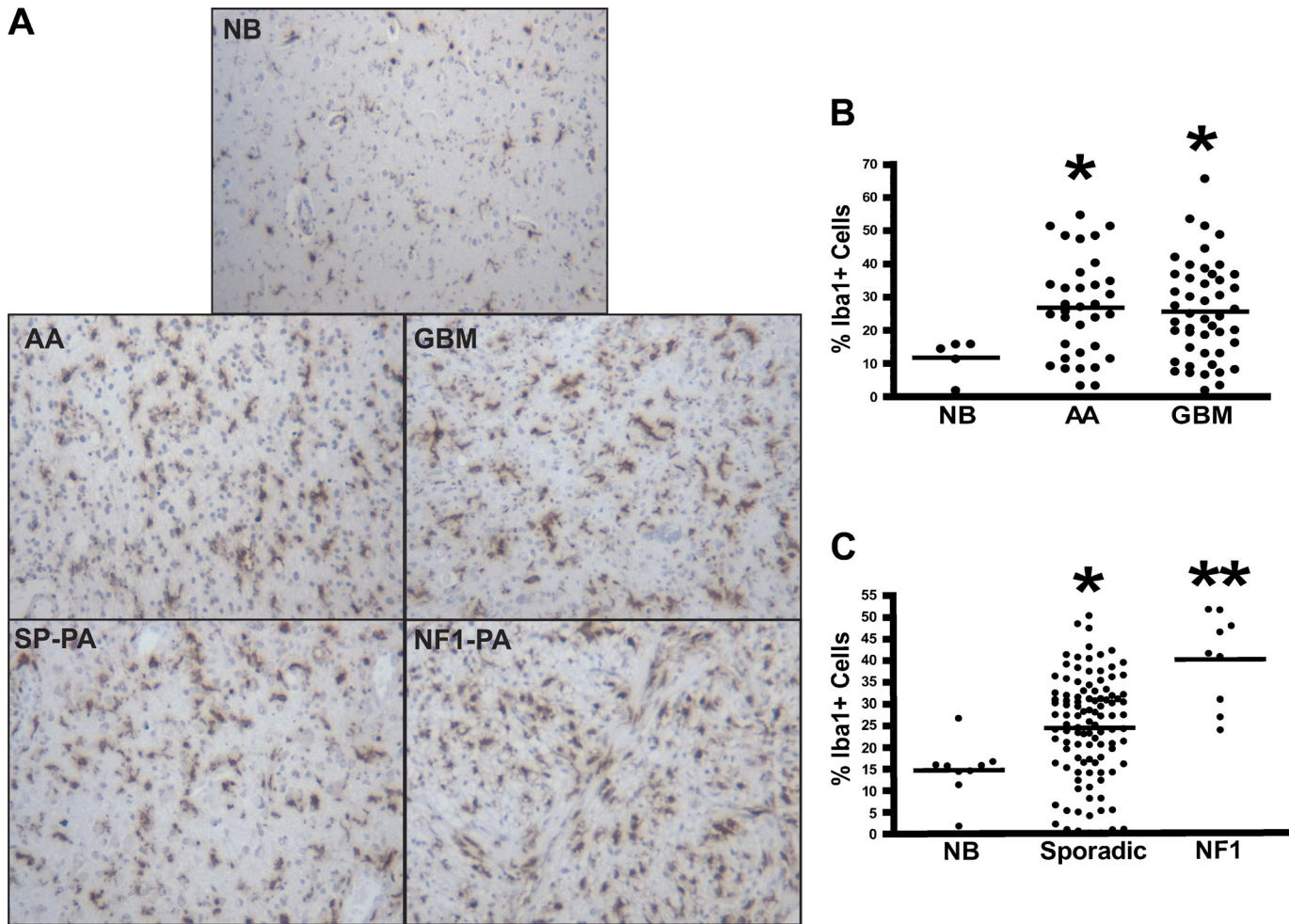


FIGURE 1. Increased microglia in neurofibromatosis type 1 (NF1)-associated pilocytic astrocytomas. **(A–C)** Iba1 immunohistochemistry demonstrates increased percentages of microglia in anaplastic astrocytomas (AA) ($p = 0.0236$) and glioblastoma multiforme (GBM) tumors ($p = 0.0377$) versus nonneoplastic brain (NB). **(C)** Sporadic pilocytic astrocytomas (SP-PA) have a greater percentage of Iba1⁺ cells compared with NB ($p < 0.0001$) **(A, C)**, but the greatest percentage of microglia is seen in NF1-associated pilocytic astrocytomas (NF1-PA) ($p < 0.0001$ versus NB) ($p = 0.0008$ versus SP-PA).

increased numbers of CD68⁺ cells in NF1-PA tumors versus both their sporadic counterparts and nonneoplastic brain (NB) tissue, the results did not reach statistical significance (Figure, Supplemental Digital Content 2, parts A, B, <http://links.lww.com/NEN/A200>). We suspect the differences between the results obtained using Iba1 and CD68 immunostaining reflects the labeling of blood-derived macrophages and neutrophils by the anti-CD68 but not the Iba1 antibody. We also observed stronger immunoreactivity with the Iba1 antibody in the formalin-fixed, paraffin-embedded specimens. Moreover, in studies of CD68 and Iba1 colabeling in areas of brain ischemia, numerous CD68⁺ cells lacked Iba1 colabeling and, therefore, likely represented bone marrow-derived macrophages, leukocytes, neutrophils, or dendritic cells (35, 39) (Figure, Supplemental Digital Content 2, part C, <http://links.lww.com/NEN/A200>). The finding of greater numbers of Iba1⁺ microglia in NF1-PA than in SP-PA raised suggested that these stromal cells play a particularly important role in NF1-associated gliomas.

Genetic Ablation of Microglia in Established Tumors Decreases *Nf1* Mouse Optic Glioma Proliferation

Our previous study on microglia in human pilocytic astrocytomas suggested that the number of microglia in the tumors positively correlated with glioma proliferation rate (42). We also previously showed that minocycline- or JNK inhibitor-mediated microglia inactivation decreased optic glioma tumor cell proliferation *in vivo* (20). However, these pharmacologic approaches are limited by potential off-target effects affecting other cell types in the tumor microenvironment and do not directly address the role of microglia in tumor proliferation. To establish a more definitive role for microglia in regulating *Nf1* optic glioma proliferation in *Nf1*^{+/−}*GFAP*^{CKO} mice at 3 months with radiographically and histologically obvious tumors (glioma maintenance), we used a novel transgenic mouse in which CD11b⁺ cells express the thymidine kinase (TK) gene (22). On the administration of GCV, CD11b⁺ cells are killed.

To characterize the CD11b⁺ population in the mouse optic nerve and to determine whether the ablated CD11b⁺ cells were primarily microglia, we performed flow cytometry and immunohistochemistry studies using several established monocyte markers. First, we found that CD11b and CD68 label the same population of cells in the optic nerves of 6-week-old WT mice (Fig. 2A). Most of this population expressed low levels of CD45 characteristic of resident microglia (R1 = 95% of the CD11b⁺ cell population) rather than high levels of CD45 indicative of bone marrow-derived macrophages (Fig. 2B). Iba1 colabeled these CD11b⁺ cells, as determined by flow cytometry (Fig. 2C) and Iba1/CD11b double labeling in optic nerve sections (Fig. 2D). In both cases, more than 99% of the cells analyzed were positive for both CD11b and Iba1. Iba1⁺ cells also express low levels of CD45 (Fig. 2E; R1 = 95% of Iba1⁺ cells), consistent with their classification as resident microglia. Moreover, using CD11b magnetic bead capture of microglia from optic gliomas of 3-month-old *Nf1*^{+/−}*GFAP*^{CKO} mice, most of the CD11b⁺ population isolated had low CD45 expression (Fig. 2F), thereby establishing that GCV/TK-mediated ablation of CD11b⁺ cells in *Nf1* mouse optic gliomas mainly targets the resident microglia population.

On the basis of these findings, we intercrossed CD11b-TK mice with our *Nf1*^{+/−}*GFAP*^{CKO} mice to generate *Nf1*^{+/−}*GFAP*^{CKO}-TK mice and injected GCV intraperitoneally daily for 2 weeks into 3-month-old *Nf1*^{+/−}*GFAP*^{CKO}-TK mice. For controls, vehicle (PBS) was injected into 3-month-old *Nf1*^{+/−}*GFAP*^{CKO}-TK mice. At the completion of the 2-week treatment, the optic nerves were removed for analysis. After GCV administration, there was a 49% reduction in the numbers of Iba1⁺ microglia in the optic nerves of the 3-month-old GCV-treated versus vehicle-treated control mice (Fig. 3A). No differences in numbers of Iba1⁺ cells or Ki67-positive cells between PBS-treated *Nf1*^{+/−}*GFAP*^{CKO}-TK mice were found compared with GCV-treated *Nf1*^{+/−}*GFAP*^{CKO} mice lacking the CD11b-TK transgene (data not shown). Consistent with previous studies using minocycline (20), GCV-mediated microglia ablation reduced optic glioma proliferation (Ki67-positive staining), by 94% (Fig. 3B). This reduction in proliferation reflects reduced glial cell proliferation and not microglia proliferation, as demonstrated by a lack of double labeling for Ki67 and Iba1 (Figure, Supplemental Digital Content 3, <http://links.lww.com/NEN/A201>) (20). In contrast to the effects of GCV treatment on microglia cell numbers and optic glioma proliferation, there was no significant change in the number of CD34⁺ cells within the optic nerves of GCV-treated *Nf1*^{+/−}*GFAP*^{CKO}-TK mice compared with vehicle-treated controls (Fig. 3C). Together with previous studies, these new findings establish a critical role for microglia in the maintenance of *Nf1* mouse optic glioma proliferation.

Microglia Ablation During Optic Glioma Development Reduces Tumor Proliferation

One of the unique opportunities afforded by GEM tumor models is the ability to define the role of stromal cell types during tumor evolution. We hypothesized that microglia might also have important functions during optic glioma formation that may be distinct from their growth-promoting role in glioma maintenance. Previously, we showed that the earliest

changes in optic nerve organization were observed between 3 and 6 weeks, as evidenced by increased numbers of microglia (20), increased glial cell proliferation (9, 26), and disruption of the relationship between optic nerve axons and their associated glia (43). To determine the impact of microglia inactivation/ablation during the early phase of optic glioma formation, we treated *Nf1*^{+/−}*GFAP*^{CKO}-TK mice with GCV or control vehicle (PBS) for 2 weeks beginning at the age of 3 weeks.

Similar to the GCV-treated 3-month-old *Nf1*^{+/−}*GFAP*^{CKO}-TK mice, there was a 43% decrease in the number of Iba1⁺ cells in the optic nerves of GCV-treated mice at 3 to 5 weeks versus controls (Fig. 4A). After GCV treatment, optic glioma proliferation was decreased by 63% (Fig. 4B), with no change in the number of CD34⁺ cells (Fig. 4C). These results demonstrate for the first time that microglia also facilitate glial cell proliferation during the early phases of optic glioma development.

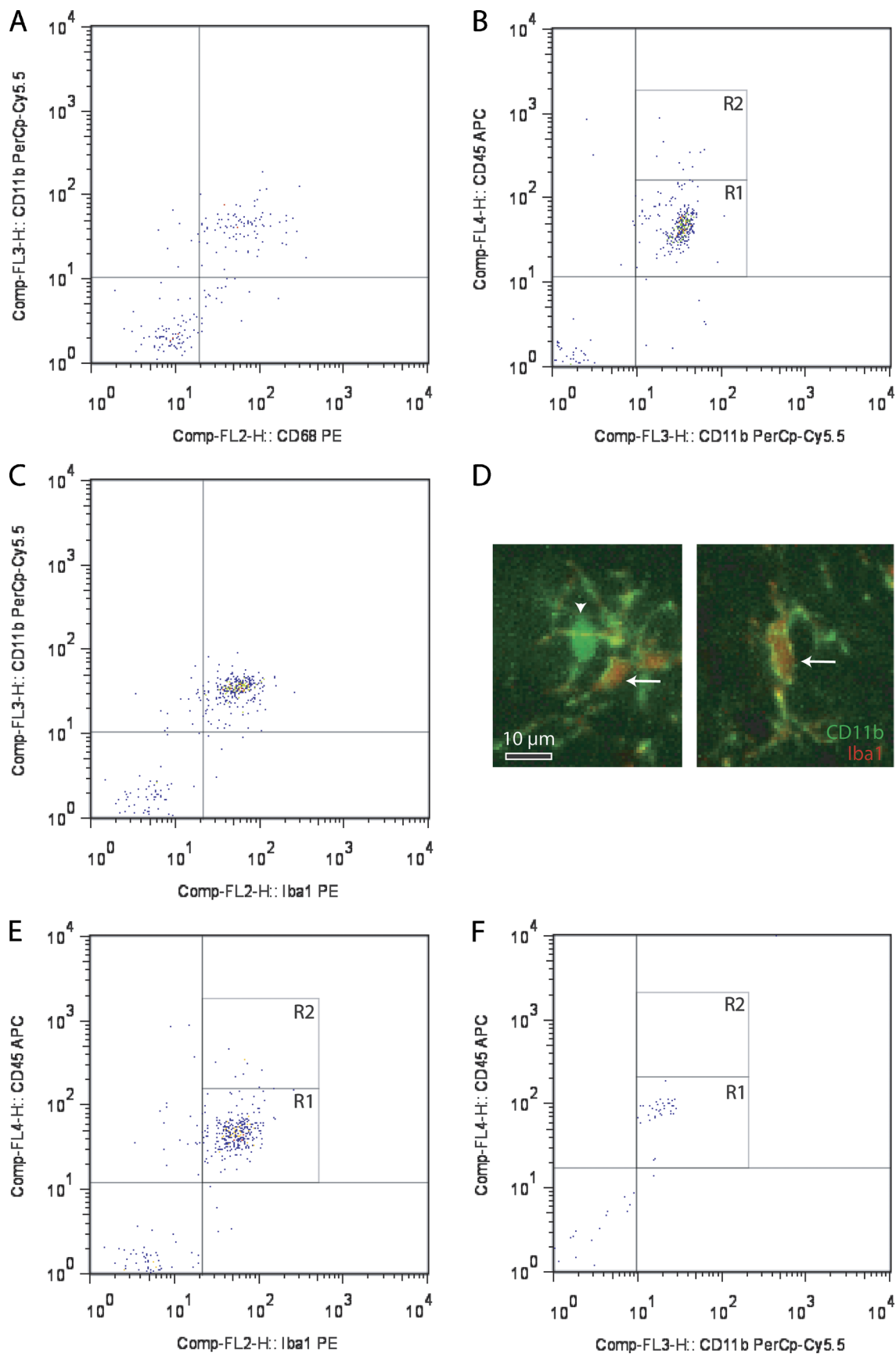
Nf1^{+/−} Optic Nerves Have Increased Numbers of Microglia at the Age of 6 Weeks But Not 3 Weeks or 3 Months

We next sought to determine whether *Nf1* heterozygosity resulted in a temporally and spatially restricted increase in microglia numbers. For these studies, we performed Iba1 immunostaining in the optic nerves and brains of *Nf1*^{+/−} and WT mice at 2 time points: before obvious glioma formation (3 weeks and 6 weeks) and a time point when radiographically and histologically evident gliomas are seen (3 months). At 3 weeks, *Nf1*^{+/−} and WT mice had equivalent numbers of Iba1⁺ cells in the optic nerve, but at 6 weeks, microglia numbers in the WT optic nerve had decreased compared with the WT optic nerve at 3 weeks, whereas the number of microglia in the *Nf1*^{+/−} optic nerve did not decline (Figs. 5A, B). This difference in microglia dispersal resulted in a 2-fold increase in the number of microglia in the optic nerves of *Nf1*^{+/−} mice compared with their WT littermates. By 3 months, no differences in optic nerve microglia numbers were observed between *Nf1*^{+/−} and WT mice (Figs. 5A, B). These results support the notion that there is developmental (temporal) regulation of microglia numbers in the optic nerve resulting from *Nf1* heterozygosity, suggesting that *Nf1*^{+/−} microglia have delayed or defective dispersion.

To determine whether this effect of *Nf1* heterozygosity on microglia number was also spatially regulated, we counted microglia in the brainstem and neocortex of the *Nf1*^{+/−} and WT mice. In striking contrast to the temporal effects of *Nf1* heterozygosity in optic nerves, no differences in brainstem or neocortex microglia numbers were observed at 3 weeks, 6 weeks, or 3 months between *Nf1*^{+/−} mice and their WT littermates (Figs. 5C, D). Thus, *Nf1* heterozygosity results in both a temporal and spatial increase in microglia within the mouse optic nerve.

CX3CR1 Expression Is Reduced in the Optic Nerves of *Nf1*^{+/−} Mice

One of the key chemokines that regulate microglia dispersal in the brain is fractalkine or CX3CL1 (44, 45).



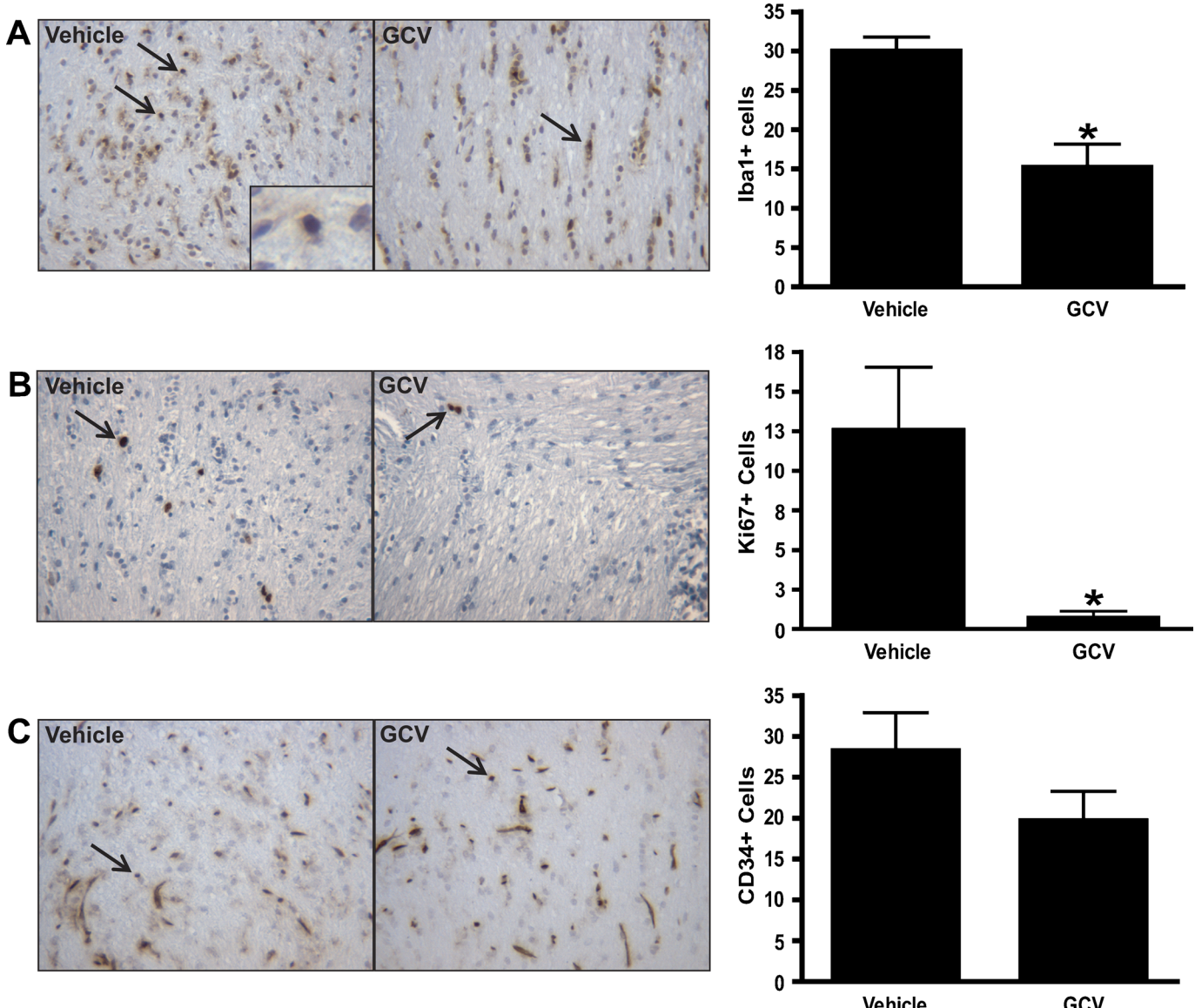


FIGURE 3. Microglia ablation at 3 months reduces optic glioma proliferation. **(A, B)** Treatment of *Nf1*^{+/-}-GFPCKO-TK mice ($n = 7$) with ganciclovir (GCV) at 3 months reduces the number of Iba1⁺ cells by 49% ($p = 0.0280$) and results in a 94% decrease in the number of Ki67-positive cells in the optic nerve ($p = 0.0118$) versus *Nf1*^{+/-}-GFPCKO-TK mice treated with vehicle ($n = 7$). **(C)** Ganciclovir treatment did not affect endothelial cell numbers, as assessed by CD34 immunohistochemistry ($p = 0.2864$).

CX3CL1 acts on its receptor, CX3CR1, to regulate microglia migration and function (46), and loss of CX3CR1 expression has been reported to lead to subretinal microglia cell accumulation (47). To determine whether altered CX3CL1/CX3CR1 expression could account for abnormal accumu-

lation of microglia in the optic nerves of 6-week-old *Nf1*^{+/-} mice, we first measured *Cx3cl1* mRNA levels by qPCR in *Nf1*^{+/-} and WT optic nerves at different ages. No differences in *Cx3cl1* expression were observed in *Nf1*^{+/-} optic nerves relative to their WT counterparts at any time point (Fig. 6A).

FIGURE 2. Microglia in the mouse optic nerve at 6 weeks and in mouse optic gliomas at 3 months are mainly resident microglia. **(A)** Flow cytometry demonstrates that most cells from 6-week-old wild-type (WT) optic nerves (10 pooled optic nerves) are doubly positive for both CD11b and CD68. **(B)** Most of these CD11b⁺ cells express low levels of CD45 (R1). **(C)** CD11b⁺ microglia in the 6-week-old optic nerve are also Iba1⁺. **(D)** Using double-labeling immunofluorescence, there are rare cells in the 6-week-old WT optic nerve that label with CD11b antibodies (green) alone (inset, arrowhead), whereas most (~99%) of the microglia colabel with both CD11b and Iba1 antibodies (inset, arrows) ($n = 5$). **(E)** Iba1⁺ cells express low levels of CD45 (R1). **(F)** CD11b magnetic cell capture of microglia from 3-month-old *Nf1*^{+/-}-GFPCKO mouse optic gliomas (7 pooled optic nerves) followed by flow cytometry demonstrates that the CD11b⁺ cells are also almost exclusively CD45^{low} (R1).

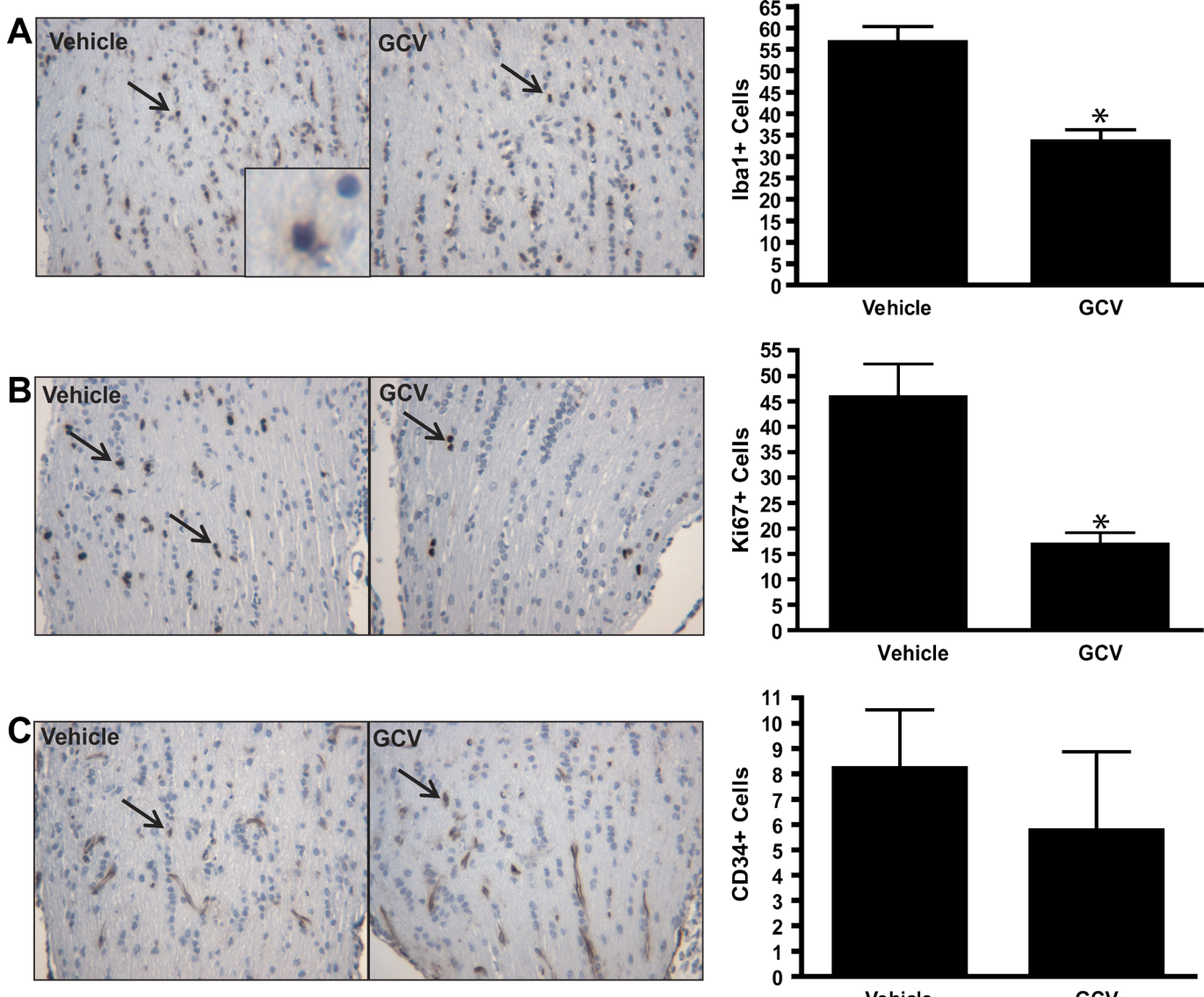


FIGURE 4. Microglia ablation at 3 weeks reduces early optic glioma proliferation. **(A, B)** $Nf1^{+/-}GFP$ CKO-TK mice ($n = 6$) treated with ganciclovir (GCV) beginning at 3 weeks reduces the number of Iba1⁺ cells by 43% ($p = 0.0012$) and results in a 63% decrease in Ki67-positive cells in the optic nerve versus $Nf1^{+/-}GFP$ CKO-TK mice ($n = 6$) treated with vehicle ($p = 0.0013$). **(C)** Ganciclovir treatment did not affect endothelial cell numbers as assessed by CD34 immunohistochemistry ($p = 0.5405$).

Next, we examined *Cx3cr1* mRNA expression by qPCR using total RNA isolated from $Nf1^{+/-}$ and WT mice optic nerves at different ages. There was a trend increase toward increased *Cx3cr1* mRNA expression at 3 weeks in $Nf1^{+/-}$ optic nerves ($p = 0.0855$), whereas there was a 2.5-fold decrease in *Cx3cr1* mRNA in $Nf1^{+/-}$ compared with WT optic nerves at 6 weeks (Fig. 6B). By 3 months, *Cx3cr1* mRNA expression in the $Nf1^{+/-}$ optic nerves was equivalent to that in the WT mice. Attempts to confirm these results at the protein level were unsuccessful owing to the lack of suitable CX3CR1 antibodies for immunohistochemistry.

To determine whether reduced CX3CR1 expression leads to increased microglia accumulation in the optic nerve as observed in $Nf1^{+/-}$ mice, we used *Cx3cr1+GFP* mice in which 1 copy of the *Cx3cr1* gene was replaced with a com-

plementary DNA encoding green fluorescent protein (GFP) (23). At 6 weeks, there were 2-fold more Iba1⁺ cells in the optic nerves of *Cx3cr1+GFP* mice compared with WT controls (Fig. 6C). Similarly, there was an increase in the number of Iba1⁺ cells in the optic nerves of $Nf1^{+/-}; Cx3cr1+GFP$ mice compared with $Nf1^{+/-}$ controls at 6 weeks ($p < 0.0001$). Collectively, these results suggest that $Nf1^{+/-}$ microglia exhibit a delay in dispersal from the optic nerve related to reduced CX3CR1 expression, resulting in increased numbers of microglia at a critical time during optic glioma development.

DISCUSSION

Gliomagenesis requires the combination of susceptible preneoplastic cells coupled with spatially and temporally

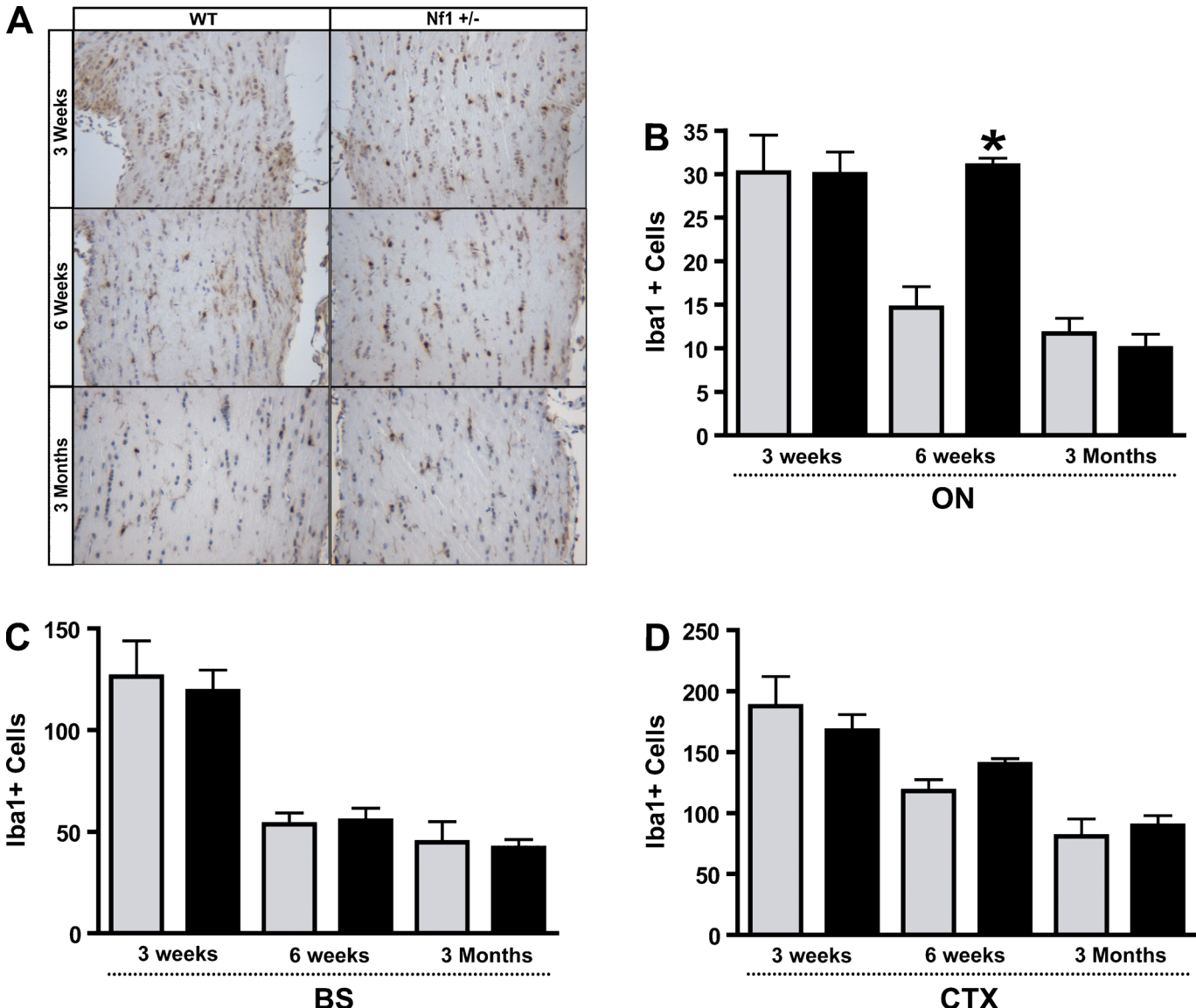


FIGURE 5. Iba1⁺ cells are increased in Nf1^{+/−} optic nerve (ON) at 6 weeks but not at 3 weeks or 3 months. **(A, B)** Equivalent numbers of Iba1⁺ cells were found in the ON of Nf1^{+/−} (n = 5) (black bars) and wild-type (WT) (gray bars) mice (n = 5) at 3 weeks ($p = 0.9712$). By 6 weeks, there was a 2-fold increase in the number of Iba1⁺ microglia in the ONs of Nf1^{+/−} mice (n = 5) versus WT littermates (n = 5) ($p = 0.0002$). By 3 months, Nf1^{+/−} (n = 4) and WT (n = 4) mice had equivalent numbers of Iba1⁺ cells ($p = 0.5155$). **(C, D)** Nf1^{+/−} mice (n = 5) have similar numbers of Iba1⁺ microglia in the brainstem (BS) and cortex (CTX) versus WT (n = 5) at 3 weeks (BS, $p = 0.7531$) (CTX, $p = 0.5248$), 6 weeks (BS, $p = 0.8260$) (CTX, $p = 0.0911$), and 3 months (BS, $p = 0.8138$) (CTX, $p = 0.6162$).

restricted signals emanating from the tumor microenvironment. This cellular collaboration may account for the unique pattern of glioma formation within the CNS in children with NF1. With few exceptions, gliomas are predominantly located along the optic pathway and less frequently in the brainstem in young children. On the basis of this unique pattern of gliomagenesis, we previously showed that optic nerve and brainstem, but not the neocortex, astrocytes increase their proliferation in response to Nf1 gene inactivation in vitro and in vivo (48). This region-specific susceptibility to the effects of neurofibromin loss provides a receptive preneoplastic cell

type, which, in cooperation with specific signals from the local environment, facilitates gliomagenesis.

The requirement for key stromal signals is illustrated by studies of Nf1 GEM strains. In both peripheral and CNS tumors, Nf1 loss in Schwann cell or glial cell precursors, respectively, is not sufficient for tumor formation (5, 7). Neurofibromas or gliomas only form when Nf1 inactivation occurs in Schwann or glial cell precursors in Nf1^{+/−} mice (5, 8, 49). The obligate role of Nf1^{+/−} cells in the process of tumor formation and continued growth is further underscored by studies that identify mast cells (3, 4, 50) and microglia (20, 21) as

important stromal cell types in neurofibroma and optic glioma development and maintenance, respectively. In the current study, we show that NF1-associated human pilocytic astrocytomas have increased numbers of microglia and use several *Nf1* GEM strains to establish a pivotal role for resident microglia in both optic glioma development and maintenance.

First, we demonstrated that astrocytic tumors of all malignancy grades harbor increased percentages of Iba1⁺ microglia versus nonneoplastic brain. Previous studies have

used CD68 or Iba1 to identify microglia and found correlations between the malignancy grade and CD68/Iba1 immunopositivity (51, 52), but others have reported differences in microglia morphology (12) or proliferation (40) in gliomas of varying histologic grade. We observed a statistically insignificant trend toward increased CD68⁺ cells in gliomas versus nonneoplastic brain. We suspect that the difference between CD68 and Iba1 as microglia markers reflects the fact that CD68 recognizes other monocyte-like cells in addition to microglia and may also stain nonmonocyte/macrophage lineage cells, especially under pathologic conditions (33, 35, 39). Indeed, we demonstrated that macrophages in an ischemic region in the human brain were strongly CD68⁺, whereas few cells in that pathological focus coincidentally labeled with Iba1. These data strongly suggest that Iba1 is a more selective marker for brain microglia (29, 30) but also highlight the need to identify additional specific markers for resident microglia.

We found that GCV-mediated reductions in microglia numbers were similar during tumor evolution (5–6 weeks) and in the established glioma (3 months). Using this method to attenuate microglia function, we provide definitive evidence for the role of microglia in glioma proliferation in established tumors and show for the first time their role in glioma proliferation during tumor formation. Although this method of microglia ablation should target only CNS microglia, several independent experiments confirmed the identity of the CD11b⁺ cells. Using flow cytometry, we found that the normal optic nerve macrophage/monocyte population is primarily composed of CD11b⁺ CD45^{low} cells, consistent with the profile of resident brain microglia (34, 53). Moreover, these microglia were CD68⁺ (by flow cytometry) and Iba1⁺ (by immunofluorescence and flow cytometry). Similar to our previous studies in human NF1-associated optic gliomas (20), the CD11b⁺ population in *Nf1*^{+/−}*GFAP*CKO mouse optic gliomas was CD45^{low} resident brain microglia. Together, these results support the conclusion that genetic elimination of resident microglia reduces optic glioma proliferation both during tumor formation and tumor maintenance.

Because of the limited reagents currently available to characterize brain microglia, it is possible that there are different populations of microglia in the optic nerve at 5 to 6 weeks and 3 months. In an analogous fashion, macrophages

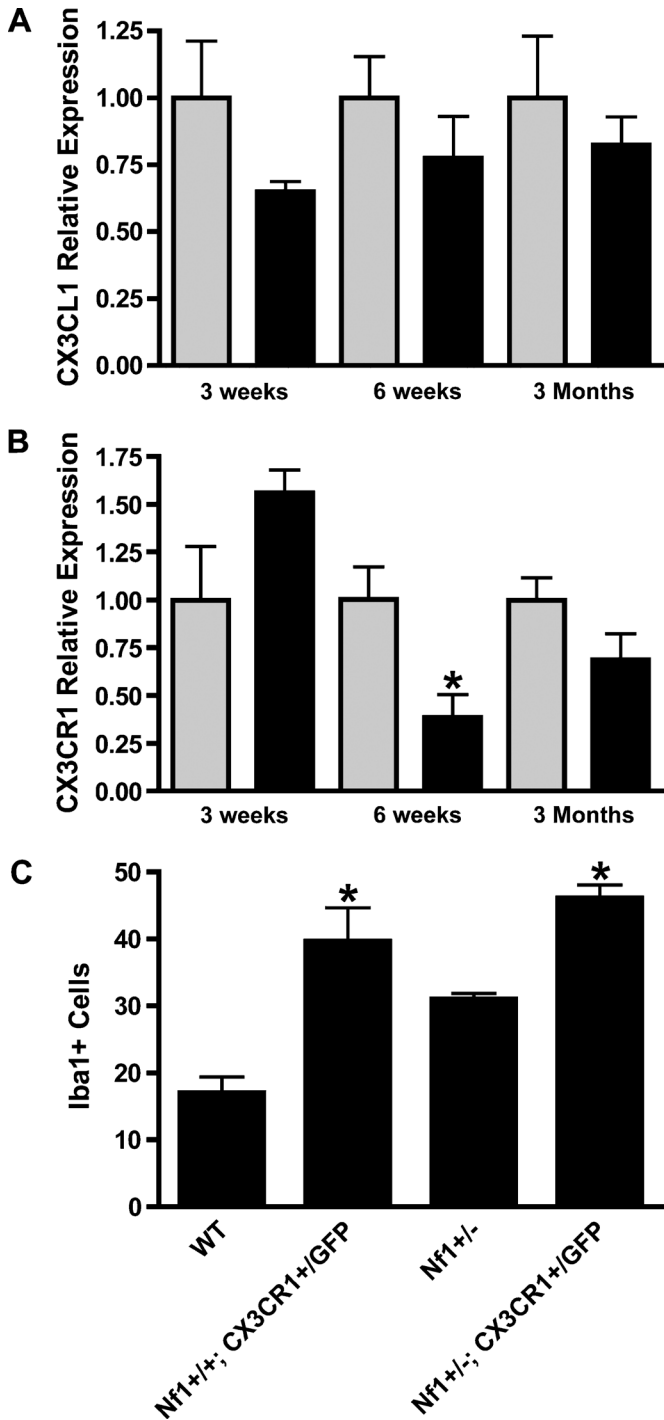


FIGURE 6. Reduced CX3CR1 expression in the *Nf1*^{+/−} optic nerve (ON). **(A)** Real-time quantitative polymerase chain reaction (PCR) reveals no change in *Cx3cl1* mRNA levels in ONs from *Nf1*^{+/−} (n = 5) (black bars) and wild-type (WT) (n = 5) (gray bars) mice at 3 weeks (p = 0.1558), 6 weeks (p = 0.3478), or 3 months (p = 0.4788). **(B)** Quantitative PCR reveals a greater than 2-fold decrease in *Cx3cr1* mRNA expression in the ONs of 6-week-old *Nf1*^{+/−} mice (n = 5) versus WT controls (n = 5) (p = 0.0181). There is no difference in *Cx3cr1* expression in the ONs from *Nf1*^{+/−} versus WT mice at 3 weeks (p = 0.0855) or 3 months (p = 0.1413). **(C)** There is a 2-fold increase in numbers of Iba1⁺ microglia in ONs of *Nf1*^{+/−} *Cx3cr1*^{+/GFP} mice (n = 6) versus WT controls (n = 5) (p = 0.0042). *Nf1*^{+/−} *Cx3cr1*^{+/GFP} mice (n = 7) have greater numbers of microglia versus WT (p < 0.0001) and *Nf1*^{+/−} mice (n = 5) (p < 0.0001).

have been proposed to have varying functions relevant to tumorigenesis as a function of tumor evolution (54, 55). Early during tumor development, macrophages are active participants in eliminating tumor cells, but as the stroma and cancer cells coevolve an “equilibrium” phase emerges in which the neoplastic cells acquire resistance to immune editing and elimination (56, 57). Finally, these “adapted” tumor cells expand and escape from immunologic pruning and create a new condition where macrophages may facilitate tumor growth. It is not clear whether these phases exist for microglia-glioma cell interactions, but if so, it will be important to identify specific subpopulations of microglia with unique properties germane to a given period of glioma development and maintenance.

We also showed that *Nf1* heterozygosity creates spatially and temporally restricted differences in microglia abundance relevant to optic glioma evolution. The fact that the numbers of Iba1⁺ microglia increase in *Nf1*^{+/−} mice in the optic nerve during a defined window of development suggests that this specific microglial population might be uniquely susceptible to the effects of reduced *Nf1* expression during this period of optic nerve maturation. We hypothesize that the accumulation of *Nf1*^{+/−} microglia in the optic nerve at 5 to 6 weeks reflects a defect in microglia homing in response to chemokines that instruct microglia dispersal. It is unlikely that *Nf1*^{+/−} optic nerve microglia have impaired migratory abilities as we have previously shown that *Nf1*^{+/−} microglia have increased motility in Boyden chamber assays *in vitro* (20, 21). Rather, we propose that *Nf1*^{+/−} microglia are defective in directed migration.

One of the major determinants controlling microglia homing is CX3CR1 (58), which was reduced in the *Nf1*^{+/−} optic nerve. Here, we showed that reduced *Cx3cr1* expression in CX3CR1-GFP heterozygous knockout mice resulted in a similar increase in optic nerve microglia at 6 weeks. These results are consistent with previous reports demonstrating that *Cx3cr1*-deficient mice exhibit microglia accumulation in the retina (47, 59, 60). Together, these findings suggest a model in which microglia accumulation reflects the impact of *Nf1* heterozygosity on the developmental pattern of microglia migration in the optic nerve, thus delaying microglia dispersal and resulting in the presence of microglia and microglia-produced signals during a time when *Nf1*^{+/−} glial progenitors are most susceptible to expansion by stromal elements.

Previous studies have demonstrated the presence of CD11b⁺, Iba1⁺, CX3CR1⁺ microglia in human gliomas, leading to the hypothesis that this cell population might be important for glioma growth (61). Moreover, polymorphisms in the human CX3CR1 gene are linked to increased survival of patients with high-grade glioma, and patients with the common “improved survival” V249I polymorphism also had reduced numbers of tumor-associated microglia (62). These findings raise the intriguing possibility that neurofibromin regulation of CX3CR1 expression might control microglia function in a specific fashion to modulate neoplastic glial cell growth in both the evolving and established optic glioma. Collectively, our new observations suggest a mechanistic model of stroma-tumor cell interaction relevant to optic gliomagenesis and maintenance that envisions *Nf1* heterozygosity as an essential event that alters microglia abundance during

optic nerve development. Future studies aimed at defining the function of microglia during gliomagenesis and glioma maintenance will be required to begin to develop treatments that target the relevant microenvironmental cell types in this common pediatric brain tumor.

ACKNOWLEDGMENTS

The authors thank Dr. Jean-Pierre Julien (Laval University) for the CD11b-TK mice used in these studies and Dr. Daniel Littman (New York University) for providing the CX3CR1-GFP mice. The authors also thank the Alvin J. Siteman Cancer Center at Washington University School of Medicine and Barnes-Jewish Hospital in St Louis, MO, for the use of the High-Speed Cell Sorter Core.

REFERENCES

- Tlsty TD, Coussens LM. Tumor stroma and regulation of cancer development. *Annu Rev Pathol* 2006;1:119–50
- Khalaf WF, Yang FC, Chen S, et al. K-ras is critical for modulating multiple c-kit-mediated cellular functions in wild-type and *Nf1*^{+/−} mast cells. *J Immunol* 2007;178:2527–34
- Yang FC, Ingram DA, Chen S, et al. Neurofibromin-deficient Schwann cells secrete a potent migratory stimulus for *Nf1*^{+/−} mast cells. *J Clin Invest* 2003;112:1851–61
- Yang FC, Chen S, Clegg T, et al. *Nf1*^{+/−} mast cells induce neurofibroma-like phenotypes through secreted TGF-beta signaling. *Hum Mol Genet* 2006;15:2421–37
- Zhu Y, Ghosh P, Charnay P, et al. Neurofibromas in NF1: Schwann cell origin and role of tumor environment. *Science* 2002;296:920–22
- Listernick R, Darling C, Greenwald M, et al. Optic pathway tumors in children: The effect of neurofibromatosis type 1 on clinical manifestations and natural history. *J Pediatr* 1995;127:718–22
- Bajenaru ML, Zhu Y, Hedrick NM, et al. Astrocyte-specific inactivation of the neurofibromatosis 1 gene (*NF1*) is insufficient for astrocytoma formation. *Mol Cell Biol* 2002;22:5100–13
- Bajenaru ML, Hernandez MR, Perry A, et al. Optic nerve glioma in mice requires astrocyte *Nf1* gene inactivation and *Nf1* brain heterozygosity. *Cancer Res* 2003;63:8573–77
- Bajenaru ML, Garbow JR, Perry A, et al. Natural history of neurofibromatosis 1-associated optic nerve glioma in mice. *Ann Neurol* 2005;57:119–27
- Rossi ML, Hughes JT, Esiri MM, et al. Immunohistological study of mononuclear cell infiltrate in malignant gliomas. *Acta Neuropathol* 1987;74:269–77
- Badie B, Schartner JM. Flow cytometric characterization of tumor-associated macrophages in experimental gliomas. *Neurosurgery* 2000;46:957–61; discussion 61–62
- Roggendorf W, Strupp S, Paulus W. Distribution and characterization of microglia/macrophages in human brain tumors. *Acta Neuropathol* 1996;92:288–93
- Streit WJ, Conde JR, Fendrick SE, et al. Role of microglia in the central nervous system's immune response. *Neurol Res* 2005;27:685–91
- Rio-Hortega PD, Asua FD. Sobre la fagocytosis en los tumores y en otros procesos patológicos. *Arch Cardiol Hematol* 1921;2:161–220
- Zhang L, Alizadeh D, Van Handel M, et al. Stat3 inhibition activates tumor macrophages and abrogates glioma growth in mice. *Glia* 2009;57:1458–67
- Mora R, Abschuetz A, Kees T, et al. TNF-alpha- and TRAIL-resistant glioma cells undergo autophagy-dependent cell death induced by activated microglia. *Glia* 2009;57:561–81
- Frei K, Siepl C, Groscurth P, et al. Antigen presentation and tumor cytotoxicity by interferon-gamma-treated microglial cells. *Eur J Immunol* 1987;17:1271–78
- Tran CT, Wolz P, Egensperger R, et al. Differential expression of MHC class II molecules by microglia and neoplastic astroglia: Relevance for the escape of astrocytoma cells from immune surveillance. *Neuropathol Appl Neurobiol* 1998;24:293–301

19. Wagner S, Czub S, Greif M, et al. Microglial/macrophage expression of interleukin 10 in human glioblastomas. *Int J Cancer* 1999;82:12–16
20. Dagnikatte GC, Gutmann DH. Neurofibromatosis-1 (*Nf1*) heterozygous brain microglia elaborate paracrine factors that promote *Nf1*-deficient astrocyte and glioma growth. *Hum Mol Genet* 2007;16:1098–112
21. Dagnikatte GC, Gianino SM, Zhao NW, et al. Increased c-Jun-NH₂-kinase signaling in neurofibromatosis-1 heterozygous microglia drives microglia activation and promotes optic glioma proliferation. *Cancer Res* 2008;68:10358–66
22. Gowing G, Vallieres L, Julien JP. Mouse model for ablation of proliferating microglia in acute CNS injuries. *Glia* 2006;53:331–37
23. Jung S, Aliberti J, Graemmel P, et al. Analysis of fractalkine receptor CX(3)CR1 function by targeted deletion and green fluorescent protein reporter gene insertion. *Mol Cell Biol* 2000;20:4106–14
24. Tibbetts KM, Emmett RJ, Gao F, et al. Histopathologic predictors of pilocytic astrocytoma event-free survival. *Acta Neuropathol* 2009;117:657–65
25. Sharma MK, Watson MA, Lyman M, et al. Matrilin-2 expression distinguishes clinically relevant subsets of pilocytic astrocytoma. *Neurology* 2006;66:127–30
26. Hegedus B, Banerjee D, Yeh TH, et al. Preclinical cancer therapy in a mouse model of neurofibromatosis-1 optic glioma. *Cancer Res* 2008;68:1520–28
27. Cardona AE, Huang D, Sasse ME, et al. Isolation of murine microglial cells for RNA analysis or flow cytometry. *Nat Protoc* 2006;1:1947–51
28. Baumgarth N, Roederer M. A practical approach to multicolor flow cytometry for immunophenotyping. *J Immunol Methods* 2000;243:77–97
29. Ahmed Z, Shaw G, Sharma VP, et al. Actin-binding proteins coronin-1a and IBA-1 are effective microglial markers for immunohistochemistry. *J Histochem Cytochem* 2007;55:687–700
30. Ito D, Imai Y, Ohsawa K, et al. Microglia-specific localisation of a novel calcium binding protein, Iba1. *Brain Res Mol Brain Res* 1998;57:1–9
31. Dick AD, Pell M, Brew BJ, et al. Direct ex vivo flow cytometric analysis of human microglial cell CD4 expression: Examination of central nervous system biopsy specimens from HIV-seropositive patients and patients with other neurological disease. *AIDS* 1997;11:1699–708
32. Sedgwick JD, Schwender S, Imrich H, et al. Isolation and direct characterization of resident microglial cells from the normal and inflamed central nervous system. *Proc Natl Acad Sci U S A* 1991;88:7438–42
33. Pulford KA, Sipos A, Cordell JL, et al. Distribution of the CD68 macrophage/myeloid associated antigen. *Int Immunol* 1990;2:973–80
34. Ford AL, Goodsall AL, Hickey WF, et al. Normal adult ramified microglia separated from other central nervous system macrophages by flow cytometric sorting. Phenotypic differences defined and direct ex vivo antigen presentation to myelin basic protein-reactive CD4⁺ T cells compared. *J Immunol* 1995;154:4309–21
35. Matsumoto H, Kumon Y, Watanabe H, et al. Antibodies to CD11b, CD68, and lectin label neutrophils rather than microglia in traumatic and ischemic brain lesions. *J Neurosci Res* 2007;85:994–1009
36. Elghetany MT. Surface antigen changes during normal neutrophilic development: A critical review. *Blood Cells Mol Dis* 2002;28:260–74
37. Eter N, Engel DR, Meyer L, et al. In vivo visualization of dendritic cells, macrophages, and microglial cells responding to laser-induced damage in the fundus of the eye. *Invest Ophthalmol Vis Sci* 2008;49:3649–58
38. Reichmann G, Schroeter M, Jander S, et al. Dendritic cells and dendritic-like microglia in focal cortical ischemia of the mouse brain. *J Neuroimmunol* 2002;129:125–32
39. Kunisch E, Fuhrmann R, Roth A, et al. Macrophage specificity of three anti-CD68 monoclonal antibodies (KP1, EBM11, and PGM1) widely used for immunohistochemistry and flow cytometry. *Ann Rheum Dis* 2004;63:774–84
40. Klein R, Roggendorf W. Increased microglia proliferation separates pilocytic astrocytomas from diffuse astrocytomas: A double labeling study. *Acta Neuropathol* 2001;101:245–48
41. Kulla A, Liigant A, Piirsoo A, et al. Tenascin expression patterns and cells of monocyte lineage: Relationship in human gliomas. *Mod Pathol* 2000;13:56–67
42. Morimura T, Neuchrist C, Kitz K, et al. Monocyte subpopulations in human gliomas: Expression of Fc and complement receptors and correlation with tumor proliferation. *Acta Neuropathol* 1990;80:287–94
43. Hegedus B, Hughes FW, Garbow JR, et al. Optic nerve dysfunction in a mouse model of neurofibromatosis-1 optic glioma. *J Neuropathol Exp Neurol* 2009;68:542–51
44. Tanabe S, Heesen M, Yoshizawa I, et al. Functional expression of the CXC-chemokine receptor-4/fusin on mouse microglial cells and astrocytes. *J Immunol* 1997;159:905–11
45. Lauro C, Catalano M, Trettel F, et al. The chemokine CX3CL1 reduces migration and increases adhesion of neurons with mechanisms dependent on the beta1 integrin subunit. *J Immunol* 2006;177:7599–606
46. Sunnergren D, Eltayeb S, Nilsson M, et al. CX3CL1 (fractalkine) and CX3CR1 expression in myelin oligodendrocyte glycoprotein-induced experimental autoimmune encephalomyelitis: Kinetics and cellular origin. *J Neuroinflammation* 2005;2:17
47. Combadiere C, Feumi C, Raoul W, et al. CX3CR1-dependent subretinal microglia cell accumulation is associated with cardinal features of age-related macular degeneration. *J Clin Invest* 2007;117:2920–28
48. Yeh TH, Lee DY, Gianino SM, et al. Microarray analyses reveal regional astrocyte heterogeneity with implications for neurofibromatosis type 1 (NF1)-regulated glial proliferation. *Glia* 2009;57:1239–49
49. Zhu Y, Harada T, Liu L, et al. Inactivation of NF1 in CNS causes increased glial progenitor proliferation and optic glioma formation. *Development* 2005;132:5577–88
50. Yang FC, Ingram DA, Chen S, et al. Nf1-dependent tumors require a microenvironment containing *Nf1*^{+/-} and c-kit-dependent bone marrow. *Cell* 2008;135:437–48
51. Strojnik T, Kavalari R, Zajc I, et al. Prognostic impact of CD68 and kallikrein 6 in human glioma. *Anticancer Res* 2009;29:3269–79
52. Deininger MH, Seid K, Engel S, et al. Allograft inflammatory factor-1 defines a distinct subset of infiltrating macrophages/microglial cells in rat and human gliomas. *Acta Neuropathol* 2000;100:673–80
53. Sedgwick JD, Hughes CC, Male DK, et al. Antigen-specific damage to brain vascular endothelial cells mediated by encephalitogenic and non-encephalitogenic CD4⁺ T cell lines in vitro. *J Immunol* 1990;145:2474–81
54. Smyth MJ, Dunn GP, Schreiber RD. Cancer immunosurveillance and immunoediting: The roles of immunity in suppressing tumor development and shaping tumor immunogenicity. *Adv Immunol* 2006;90:1–50
55. Bui JD, Schreiber RD. Cancer immunosurveillance, immunoediting and inflammation: Independent or interdependent processes? *Curr Opin Immunol* 2007;19:203–8
56. Uhr JW, Scheuermann RH, Street NE, et al. Cancer dormancy: Opportunities for new therapeutic approaches. *Nat Med* 1997;3:505–9
57. Wheelock EF, Weinhold KJ, Levich J. The tumor dormant state. *Adv Cancer Res* 1981;34:107–40
58. Zhu J, Zhou Z, Liu Y, et al. Fractalkine and CX3CR1 are involved in the migration of intravenously grafted human bone marrow stromal cells toward ischemic brain lesion in rats. *Brain Res* 2009;1287:173–83
59. Liang KJ, Lee JE, Wang YD, et al. Regulation of dynamic behavior of retinal microglia by CX3CR1 signaling. *Invest Ophthalmol Vis Sci* 2009;50:4444–51
60. Raoul W, Keller N, Rodero M, et al. Role of the chemokine receptor CX3CR1 in the mobilization of phagocytic retinal microglial cells. *J Neuroimmunol* 2008;198:56–61
61. Held-Feindt J, Hattermann K, Muerkoster SS, et al. CX3CR1 promotes recruitment of human glioma-infiltrating microglia/macrophages (GIMs). *Exp Cell Res* 2010;316:1553–66
62. Rodero M, Marie Y, Couderet M, et al. Polymorphism in the microglial cell-mobilizing CX3CR1 gene is associated with survival in patients with glioblastoma. *J Clin Oncol* 2008;26:5957–64